Kinetics and Catalysis, Vol. 38, No. 4, 1997, pp. 565–573. Translated from Kinetika i Kataliz, Vol. 38, No. 4, 1997, pp. 617–625.

Study of Oxygen Adsorption on Ag/α-Al_2O_3 Catalysts under Ultrahigh/High Vacuum Conditions

S. N. Trukhan, V. P. Ivanov, and B. S. Bal'zhinimaev

Boreskov Institute of Catalysis, Siberian Division, Russian Academy of Sciences, Novosibirsk, 630090 Russia

Received March 18, 1996

Abstract—Adsorption of oxygen on Ag/α-Al_2O_3 catalysts with mean sizes of silver particles of 160, 560, and 1000 Å is studied by thermal desorption at 300–500 K and pressures below 10^{-2} Pa and in the range 500–15 000 Pa. It is found that for both initial catalysts and those activated under the conditions for ethylene epoxidation, several forms of oxygen thermal desorption are observed: molecular (T_{max} = 350–400 K), atomic (560–580, 700 K), and the form caused by the penetration of oxygen into subsurface layers (610–630 K). The kinetics and parameters of oxygen adsorption on small particles qualitatively and quantitatively differ from those on the species of a large size. A kinetic scheme that explains the temperature dependence of the initial sticking coefficient of oxygen is suggested for the dissociative adsorption of oxygen. The amount of molecular oxygen adsorbed can be considered as a measure of defects (roundness) on the surface of silver particles.

INTRODUCTION

The interaction of oxygen with a silver surface has attracted a keen interest, first of all, because silver exhibits unique catalytic properties in ethylene epoxidation. This fact and the rapid progress in development of experimental techniques for studying surface processes have stimulated the intensive studies of oxygen adsorption on silver in the last two decades [1–10].

Having generalized a great body of data, one can draw a conclusion that at low oxygen pressures ($P_{O_2} \leq 10^{-2}$ Pa) and temperatures of 400–500 K, oxygen is adsorbed on silver dissociatively, and the spectrum of oxygen thermal desorption (TD) exhibits a peak at $T_{max} \sim$ 550–600 K. This state of oxygen was observed on single crystals of different orientation [1–4], polycrystalline samples [5, 6], silver powder [7], and supported catalysts [8]. The rate of formation of this state in the course of oxygen adsorption strongly depends on the nature of the defects at a surface. Thus, the initial sticking coefficient (S_0) at $T_{ads} \sim$ 470 K on a close-packed (111) plane is 10^{-5}–10^{-6}, and it equals 10^{-4} on a more "open" (110) plane [1–4]. As was shown by field-emission microscopy, the rate of oxygen adsorption is the highest on a the "rough" (201) plane [9]. An increase in a number of defects on Ag(111) plane after ion bombardment results in an increase in the adsorption rate by an order of magnitude [10]. For silver powder and the Ag/α-Al_2O_3 catalyst, their surfaces being represented mostly by the (111) planes with a high density of steps and defects, the value $S_0^{470\,K} \sim 10^{-5}$ was obtained [7, 8].

In addition to the dissociatively adsorbed oxygen, the molecular form of oxygen characterized by the desorption peak at 350–400 K was observed on the Ag(111) plane [2], on silver wire [5], on supported [11], and unpromoted promoted catalysts [12, 13].

At elevated temperatures and O_2 pressures, adsorption of oxygen by subsurface silver layers was observed by many authors. This form of oxygen is desorbed in the temperature range from 650 to 850 K, depending on the adsorption conditions and the structure of the surface [5, 6, 11, 14]. It is noted that the subsurface state of oxygen is typical of supported silver catalysts rather than bulk silver [15].

The role of these three states of oxygen in ethylene oxidation consists in the following. Chemisorbed atomic oxygen reacts with ethylene to give both ethylene epoxide and the products of complete oxidation of ethylene [6, 16], whereas molecular oxygen takes no part in ethylene oxidation because of the low heat of adsorption [16]. The existence of subsurface oxygen appears to be necessary but insufficient for ethylene epoxidation to occur [6, 16, 17].

In this work, adsorption of oxygen on Ag/α-Al_2O_3 catalysts with different dispersion is studied at T = 300–470 K and oxygen pressures of 5×10^{-3}–10^{-2} and 500–15 000 Pa. We made an attempt, first, to elucidate the effect of the silver particle size on the kinetics and forms of oxygen adsorption; second, to study the state of oxygen on the catalysts of ethylene epoxidation; and, third, to understand how the difference in adsorption properties of samples may be responsible for the effect of the particle size on the change in the ethylene epoxidation rate by more than an order of magnitude [18]. To

0023-1584/97/3804-0565$18.00 © 1997 МАИК Наука /Interperiodica Publishing

Characteristics of $Ag/\alpha\text{-}Al_2O_3$ catalysts*

d	C	S_{sp}	v
160	0.41	0.15	0.2
560	5.2	0.52	6.3
1000	13.8	0.62	4.8

* d is the mean silver particle size, Å; C is the silver content, wt %; S_{sp} is the silver specific surface area, m^2 Ag/g Cat; v is the ethylene epoxidation rate $\times 10^{-17}$, C_2H_4 molecules m^2Ag s^{-1}.

solve the above problems, we (1) used a set of silver catalysts with a narrow particle size distribution, namely, 160, 560, and 1000 Å (the deviation from the mean value is within ±20%), (2) comprehensively characterized the structure and electronic properties of silver in the samples by NMR [19], HREM, XRD [20], and XPS [21], and (3) applied rapid temperature-programmed desorption specially developed for the quantitative mass-spectrometric analysis of small powdered samples (~2 mg/cm^2).

EXPERIMENTAL

Preparation of Catalysts

Silver catalysts with a narrow particle size distribution were prepared by impregnation of $\alpha\text{-}Al_2O_3$ (S_{sp} = 7 m^2/g) with silver amine complexes followed by low-temperature adsorption–contact drying. The samples reduced in a vacuum at 363 K were washed with bidistilled water several times, dried at 373 K, and calcined at 513 K in air for 2 h. The silver content in catalysts was determined by atomic absorption spectroscopy. The size of silver particles was determined by electron microscopy using a JEM-100 instrument and by oxygen chemisorption. The procedure for preparing the support and catalysts, as well as their characteristics, are described in greater detail elsewhere [18]. Some parameters of $Ag/\alpha\text{-}Al_2O_3$ samples are listed in the table.

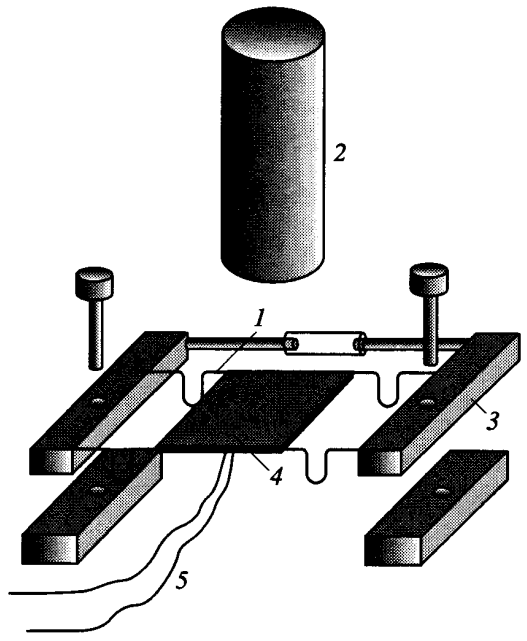

Fig. 1. Diagram of the separating part of the manipulator: (*1*) tungsten wires; (*2*) ion source and mass spectrometer; (*3*) holding frame (steel, glass); (*4*) tantalum foil; (*5*) W–Re thermocouple.

Procedure

Experiments were carried out in a metallic vacuum setup (the chamber volume was 2.3×10^3 cm^3) supplied with an MX-7304 monopolar mass-spectrometer (1–250 amu) and Penning ion pressure transducer. The pressure of residual gases, mainly H_2O, remained after annealing the setup at 373 K for 1 h was no higher than 10^{-5} Pa. The experiments showed that these conditions were sufficient for "clean off reactions," i.e., the reactions of O_{ads} with the molecules of residual gases (mainly CO), almost do not occur upon the adsorption of oxygen. The mass sweep and data processing were controlled by a DVK-3 computer coupled with the mass-spectrometer via a KAMAK module system for process control. Computer program provided the multiple cyclic measurement of ion currents of certain masses during one TD run (up to twelve masses in a cycle).

A 3.1-g holder that can be separated from a manipulator was constructed to perform thermal desorption experiments with powdered substances (Fig. 1). The holder represented a tantalum foil 0.5 mm in thickness and 10×8 mm^2 in area spot-welded between two tungsten wires 0.3 mm in diameter. The ends of the wires were, in their turn, welded to steel bars, which were screwed to the manipulator. The foil was placed in line with the mass-spectrometer ion source to ensure a straight flight of analyzed molecules.

A uniform layer of the *n*-heptane suspension of a catalyst preliminarily ground in a mortar was supported using a syringe onto the tantalum foil. The weight of a sample (usually 2–3 mg) was found by weighing the holder before and after supporting by catalyst.

The tungsten wires, to which tantalum foil was attached, were heated by passing the current. Both the foil and the sample were also heated because of the high heat conductivity of the foil. The foil temperature was measured by a W–Re (5% W and 20% Re) thermocouple spot-welded to the foil. The rate of heating was ~1.5 K/s.

The heating time constant of the tantalum foil τ can be evaluated from the following relation: $\tau \sim h_1^2/\alpha$, where $\alpha = \lambda/c\rho$ is the thermometric conductivity; λ is the heat conductivity; c is the heat capacity; ρ is the density; and h_1 is the half-width of the foil (4 mm). Substituting the corresponding values taken from [22] in

the above expression, one gets $\tau_{Ta} \approx 0.7$ s for the tantalum foil. The catalyst supported on the foil is a porous substance, and its heating time constant is described by the formula $h_2^2 c\rho/\lambda_{eff}$, where h_2 is the thickness of the supported catalyst layer (~20 μm); λ_{eff} is the effective heat conductivity of a porous substance that can be found by the formula [23]

$$\lambda_{eff} \approx \frac{\lambda}{h/2r + \ln(h/r)/\pi},$$

where $h \sim 1.1 \times 10^{-7}$ m is the mean size of the support particles and r is the radius of the spot formed by contacting particles. Assuming $r = 10^{-10}$ m, we get $\tau_{sam} = 10^{-2}$ s. This is an upper limit of τ_{sam}, because the radius of the spot formed by contacting particles is obviously greater than the typical atomic size, and, therefore, the heating time constant of the catalyst should be shorter than 10^{-2} s.

Because $\tau_{sam} \ll \tau_{Ta}$, one can draw a conclusion that within a good accuracy, the temperature of a catalyst on the support equals the temperature of the tantalum foil measured by the thermocouple. The fact that the value of τ_{max} for the desorption of chemisorbed oxygen (560 K) is in good agreement with the data obtained for bulk silver samples [1–7] supports the correctness of such a conclusion.

The kinetics of oxygen adsorption was studied with initial and activated catalysts. Activated catalysts are defined as the catalysts, which were treated at $T = 503$ K in a flow-circulation setup first with a mixture containing 7% of oxygen and 93% of nitrogen, and then with a reaction mixture consisting of 2% of ethylene, 7% of oxygen, and 91% of nitrogen (conversion did not exceed 10%) until a steady state was reached (usually, after 6–7 h) [18].

To prepare the samples for thermal desorption experiments, they were first annealed for 30 min in oxygen at 650 K and a pressure of 5×10^{-2} Pa and then for 15 min in a vacuum at 800 K. Usually, such a treatment was repeated 3–5 times for initial catalysts and once or twice, for activated catalysts. These pretreatments resulted in similar regularities exhibited by both initial and activated catalysts in adsorption–desorption processes. To avoid the sintering of silver particles, the samples were not heated above 800 K during the thermal desorption. Note that, contrary to initial catalysts, the activated samples were first heated to 800 K in a vacuum without any pretreatment and control of the desorption products.

RESULTS

TD spectra of oxygen adsorbed at low pressures (5×10^{-4}–10^{-2} Pa) and $T_{ads} = 300$ K are presented in Fig. 2. Two desorption peaks, α and β, at $T_{max} = 350$ and ~560–580 K, respectively, were observed in the spectra of all samples. TD spectra of oxygen for the samples with

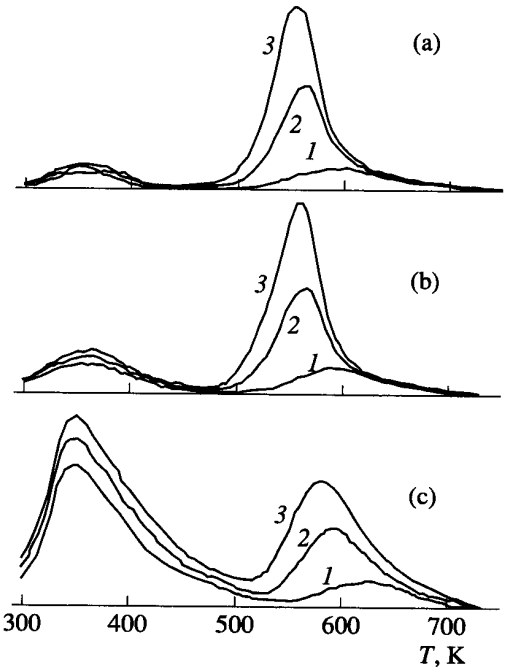

Fig. 2. TD spectra of oxygen for the samples with a silver particle size of (a) 1000, (b) 560, and (c) 160 Å obtained after oxygen adsorption at low pressures and 300 K. The coverage of the oxygen β state over the silver surface is (*1*) 0.1×10^{18}, (*2*) 0.3×10^{18}, and (*3*) 0.5×10^{18} O atoms/m^2 Ag.

large (1000 Å) and medium (560 Å) silver particles hardly differed from each other, whereas in the spectrum of the sample with small silver particles (160 Å), the β peak was significantly broadened and shifted to higher temperatures by ~20 K. Additionally, small silver particles adsorbed a much greater amount of oxygen to give the α state as compared to large particles. It is seen from Fig. 2 that for the samples with small silver particles, the coverage by oxygen in the α state was about 5 and 10 times higher than that for the samples with medium and large silver particles, respectively.

Under the conditions used for adsorption ($T_{ads} = 470$ K, $P_{O_2} < 10^{-2}$ Pa), the highest attainable coverage of the surface with oxygen in the β state was found to be equal (within the limits of 20%) for the samples with silver particles of any size. This value was virtually independent of the adsorption temperature for the particles with $d = 560$ and 1000 Å. However, for small silver particles, it decreased markedly with decreasing temperature, and at 300 K, the maximum coverage was half that found at 470 K. Unfortunately, we failed to determine the exact absolute value of the maximum coverage because of the problems associated with the calibration of pressure transducers. Nevertheless, the rough estimate gave a value of $(1–3) \times 10^{18}$ O atoms/m^2 Ag ($T_{ads} = 470$ K), this was less than a monolayer coverage for (111) and (110) planes of Ag, which is 5.67×10^{18} O atoms/m^2 Ag [3]. According to the estimate the

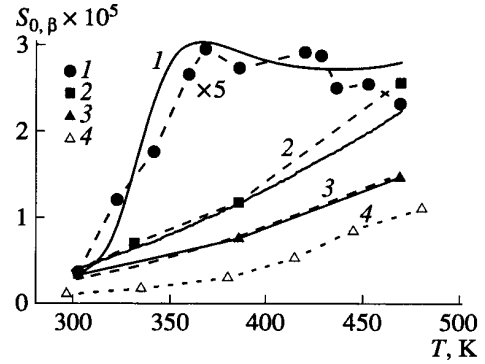

Fig. 3. Temperature dependences of $S_{0,\beta}$ for the samples with a silver particle size of (*1*) 160, (*2*) 560, and (*3*) 1000 Å. Solid lines refer to the calculated values and (*4*) are S_0 values taken from [8] (the size of particles is ~16000 Å).

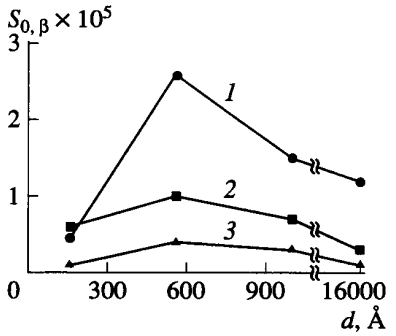

Fig. 4. Dependence of $S_{0,\beta}$ on the particle size. Adsorption temperatures are (*1*) 470, (*2*) 370, and (*3*) 300 K.

maximum attainable coverage of the surface particles with d = 160 Å by oxygen in the α state at T_{ads} = 300 K was three times greater than that for the β state at the same T_{ads}. The amount of oxygen that can be desorbed from the catalyst surface upon evacuating the vacuum chamber after the exposure at 300 K for 30 s was as great as the amount of oxygen desorbed during the following temperature-programmed heating. For this reason, the area of the α peak in Fig. 2c is only 1.5 rather than 3 times larger than the area of the β peak.

Temperature dependences of the initial sticking coefficients of oxygen adsorbed in the β state, $S_{0,\beta}$, for different samples are given in Fig. 3. Note that the $S_{0,\beta}$ values at each temperature were determined by graphical differentiation of θ(ε) curves, where ε is the exposure to oxygen, at the origin of coordinates. To improve the accuracy of determining $S_{0,\beta}$, these curves were plotted using at least six points. A similar procedure for determining the initial sticking coefficient of oxygen adsorbed in the α state, ($S_{0,\alpha}$), was much more difficult, because even at 300 K, the isothermal desorption occurred at a marked rate. Nevertheless, $S_{0,\alpha}$ was estimated at the value two orders of magnitude greater than $S_{0,\beta}$, i. e., $S_{0,\alpha} \sim 10^{-3}$.

The values of $S_{0,\beta}$ obtained for the samples with d = 560 and 1000 Å were somewhat higher (Fig. 3) than those reported in [8], where adsorption of oxygen was also studied on the supported silver particles. Unfortunately, the size of silver particles is not given in this indication. Using the values of the specific surface area and the silver content in the catalyst given in [8] and assuming the spherical shape of particles, we estimated the mean size of particles (d) at ~ 16 000 Å. As can be seen from Fig. 4, a decrease in the size of silver particles from 16 000 to 560 Å results in an increase in the initial sticking coefficient over the whole temperature range in the order $S_0^{16000\,Å} < S_0^{1000\,Å} < S_0^{560\,Å}$. As was already mentioned, this effect can be explained by an increase in the number of defects on the surface with a decrease in the particle size. Because S_0 is about ~ 10^{-6} for Ag(111) and is equal to or larger than 10^{-4} for all other planes, it is most probable that the surfaces of medium and large silver particles, for which $S_{0,\beta}$ at 470 K is 15×10^{-6} and 26×10^{-6}, respectively, represent mainly, the (111) plane with a rather high density of steps and defects.

When passing to small particles, no increase in the initial sticking coefficient was observed, contrary to what might be expected. In contrast, it dropped essentially; at 470 K, it decreased by a factor of five (Fig. 4). Note that such a decrease in the rate of oxygen adsorption on small particles correlates with a drastic drop in the reaction rate (see the table).

The adsorption of oxygen at 470 K and high pressures results in the appearance of high-temperature peaks in TD spectra. As an example, oxygen TD spectra of the sample containing silver particles with d = 1000 Å obtained after a 15-min exposure to oxygen at a pressure of 5000 Pa are given in Fig. 5. At these pressures, several TD peaks at ~560 (β), ~610 (β_1), and ~690 K (β_2) are observed. It is seen from Fig. 5 that the same states of adsorbed oxygen were observed in TD spectra of the catalyst activated under the reaction conditions as those found in the case of oxygen adsorption in a vacuum. T_{max} of desorption peaks virtually coincide in both spectra.

To answer the question whether the exchange between the low-temperature β and high-temperature β_1 and β_2 states took place, the following experiment was performed. The sample containing silver particles with d = 1000 Å was exposed to a mixture enriched to 90% in ^{18}O for 5 min at low pressures (5×10^{-3} Pa, T = 473 K). Under these conditions, only the β state was filled with ^{18}O, and then, adsorption of light oxygen was carried out at the same temperature and at a pressure of 5000 Pa, i.e., under the conditions when the β_1 and β_2 oxygen states were formed. The following thermal desorption demonstrated the presence of $^{16}O^{18}O$ in high-temperature states (Fig. 6). The amount of $^{34}O_2$

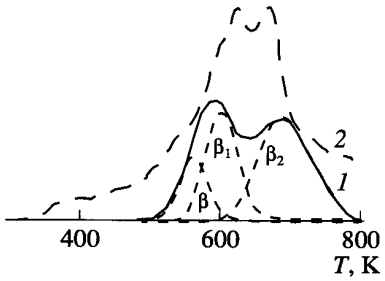

Fig. 5. TD spectra of oxygen for the sample with d = 1000 Å obtained (*1*) after oxygen adsorption at a pressure of 5000 Pa and T_{ads} = 470 K and (*2*) after activation under reaction conditions.

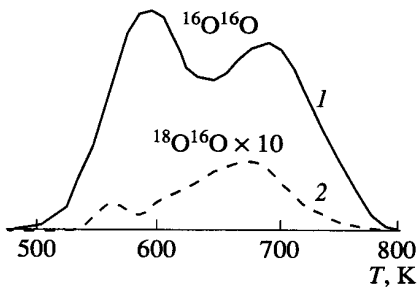

Fig. 6. TD spectra of (*1*) $^{32}O_2$ and (*2*) $^{34}O_2$ obtained after the successive treatment of the sample with d = 1000 Å by $^{36}O_2$ and $^{32}O_2$ as described in the text.

with the molecular weight 34 was essentially larger in the β_2 state than in the β_1 and β states.

A further increase in the oxygen pressure to 15000 Pa resulted in the appearance of only high-temperature species of oxygen, which exhibited desorption peaks in the temperature range from 600 K up to the silver melting point. It is important to note that the accumulation of a great number of high-temperature oxygen species led to a significant drop in the rate of oxygen adsorption with the formation of the β state. We failed to detect this state even at an exposure of 10^5 L, where 1L = 10^{-6} torr/s. The adsorption rate approached its previous value only after a prolonged annealing of silver in a vacuum.

DISCUSSION

It follows from the data reported in this work that the adsorption regularities observed for supported silver particles with a size larger than 500 Å correspond to those observed for bulk silver samples. First of all, our data on the energy characteristics of the β state (T_{max} = 560–580 K) coincide with those reported in the literature and assigned by the majority of authors to the chemisorbed oxygen species, which is close in its properties to the oxygen atoms of the surface Ag_2O phase.

The TD peak of β-oxygen (Figs. 2a, b) is well described (the standard deviation is 3–5%) by the second-order equation $d\theta/dt = \nu\theta^2\exp(-E_{des}/kT)$ with $\nu = kN_c = 10^{13}$ s^{-1} and E_{des} = 170 kJ/mol, where N_c is the number of adsorption centers per unit of surface area, 5.67×10^{18} m^{-2} [3] (in this case, the value of k falls into the range of normal values for the second-order desorption constants equal to 10^{-8}–1 m^2/s). E_{des} is close to the oxygen adsorption heats measured on single crystals and silver powders. Additionally, the temperature dependence of the initial sticking coefficient is expressed by the formula $S_0 = A\exp(-E_{des}/kT)$, and S_0 is close within an order of magnitude to that obtained for the closest-packed Ag(111) plane.

However, in going to small Ag particles (d = 160 Å), one can observe significant deviations from the classical behavior. The appearance of the α state of oxygen, which dominates in the TD spectra (Fig. 2), is one of these deviations. The activation energy of desorption determined for this state by the Readhead's procedure [24] is 92 kJ/mol, which is almost twice smaller than that obtained for the chemisorbed β state. Such a low energy of oxygen binding to the silver surface, which is not typical of the dissociative form of adsorption, and the previously revealed absence of isotope exchange for the state of oxygen with the same T_{max} of desorption [2, 13] allows one to believe that this state is formed due to adsorption of molecular oxygen. In addition, for small particles, energy characteristics for the interaction of atomic oxygen with silver also changed. The broadening of the β peak observed for small particles cannot be explained by the lateral interaction of adsorbed oxygen atoms. Indeed, if the interaction were attractive, a drastic drop in the rate of oxygen desorption would be observed at temperatures higher than T_{max} [25, 26]. If the interaction were repulsive, the broadening of the peak toward higher temperatures would occur simultaneously with the shift of its maximum to the opposite direction [26]. We managed to get a satisfactory description of the β-oxygen desorption only when the dependence of the activation energy of desorption on the coverage, $E_{des}(160\text{ Å}) = (186–10\theta)$ kJ/mol, was introduced. Formally, this dependence may indicate a higher energy inhomogeneity of the surface of small particles as compared with that of large particles. Finally, in going to small Ag particles, a sharp, fivefold decrease in $S_{0,\beta}$ (Fig. 4) is observed, and its temperature dependence, $S_{0,\beta}(T)$, no longer obeys the exponential law (Fig. 3).

Most probably, such drastic changes in the parameters of O_2 adsorption on small particles are due to essential changes in the electronic and structural properties of silver surface layers as compared to the bulk metal. Indeed, XPS studies of the same samples demonstrate that a defective phase is formed in the subsurface layer when the size of particles is smaller than 500 Å. This phase differs from bulk samples in conductivity [21]. The disappearance of the ^{109}Ag NMR signal (Knight's shift) caused by the effect of defective surface layers on

the electronic properties of the metal bulk was observed in the same range of particle sizes [19]. The above-mentioned effects result in a 20-fold decrease in the rate of epoxidation (see the table) [18]. This was explained by a sharp decrease in the fraction of the regular silver surface capable of adsorbing oxygen with the formation of a surface oxide and of activating ethylene via the formation of its π-complex with Ag^+.

Therefore, one can conclude that the structure and morphology of surface layers changed from mostly regular (flat) to virtually completely defective (rounded) with a decrease in the particle size. This change was especially sharp in the narrow range of particle sizes near 500 Å. Thus, this phenomenon is believed to be due to a drastic change in the adsorption characteristics of oxygen, in particular, to the appearance of the α state. In this case, the area of the α peak can characterize the fraction of rounded sites at the particle surface. It is seen from Fig. 2 that the area of the α peak increases sharply with an increase in the dispersion of silver. Thus, for the particles with d = 160 Å, it was five and ten times higher than for the particles with d = 560 and 1000 Å, respectively.

We made an attempt to explain the experimental dependences $S_0(T)$ obtained for different particles by the model of oxygen dissociative adsorption occurring via a molecular preadsorption state [3, 27]. It was assumed that the particle surface consisted of the sites of two types, I and II. I denoted flat sites of the particle surface with an orientation close to the (111) plane, and II denoted rounded sites, where Ag atoms had the local environment different from that in bulk samples (so-called "roughened" surface). Adsorption of oxygen proceeded on sites I via the molecular state with E_{des} = 50 kJ/mol (m_1) [3], and on defective sites, via the molecular α state (m_2) observed in this work. The diffusion of molecular and atomic oxygen between sites I and II was taken into account as a reversible reaction.

As a result, the kinetic scheme can be written as follows:

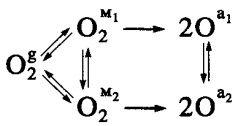

(I)

Here, O^{a_1} and O^{a_2} represented the β states of oxygen adsorbed on the regular and defective surfaces, respectively. Procedures for the calculation and determination of parameters are described below. The calculated dependences $S_0(T)$ are given in Fig. 3. As can be seen from Fig. 3, experimental data agree fairly well with those obtained within the framework of the suggested model.

At high oxygen pressures, the fraction of the β state essentially decreased, and the fractions of the high-temperature β_1 and β_2 states markedly grew. The maximum temperature of the β_2 desorption peak raised from 670 to 690 K as the O_2 pressure increased from 500 to 5000 Pa, and the area of this peak also markedly increased (doubled). A similar effect was observed on polycrystalline samples [14, 28]. The comparison of our data with those obtained in the latter works suggests that the β_2 peak corresponds to the "covalent" (electrophilic) state of oxygen. This oxygen form is localized on defective sites of the surface, the increase in the O_2 pressure favored a further increase in defectivity and, therefore, a growth in the amount of "covalent" oxygen [28]. A growth in the degree of "roughening" the surface with increasing O_2 pressure was explained by the stabilization of silver defective states by adsorbed oxygen. Recently [29], the process of "roughening" the surface of Ag(110), which proceeded under an elevated O_2 pressure and resulted in the appearance of extended "pits" and "channels" on the smooth surface, was observed by *in situ* scanning tunnelling microscopy (STM). The importance of "covalent" oxygen for the epoxidation of ethylene is obvious: this oxygen directly interacts with an ethylene molecule to form ethylene oxide [30]. However, the β_2 state on supported catalysts, in contrast to polycrystalline foil, appeared under milder adsorption conditions and desorbed somewhat earlier. For instance, in the case of the sample with d = 1000 Å, this state was formed at T_{ads} about 100 K lower. Apparently, this was due to the fact that because of the size effect [18, 19, 21], dispersed silver already contained the sufficient number of defective (rounded) sites at the surface necessary for the formation of the β_2 state.

Another significant difference is that one more β_1 state, which was not observed in TD spectra of bulk samples, appeared in TD spectra of supported silver. The fact that T_{max} in TD spectra of oxygen chemisorbed on small Ag particles (Fig. 2) is close to the position of the β_1 peak observed for large particles (Fig. 5) attracts attention. Because surface layers of small silver particles are virtually completely defective and the high-temperature state β_1 appeared on large particles only at elevated O_2 pressures and at temperatures when the surface becomes more defective, we can assume that we deal with the same state of oxygen, i.e., O^{a_2} in scheme I is identical to β_1. The nature of this state will be discussed later.

Isotope experiments (Fig. 6) clearly point to the efficient transfer of the ^{18}O label from the β to β_1 and β_2 states and that of ^{16}O back to the β state. Because $^{32}O_2$-to-$^{34}O_2$ ratios in different states are $\frac{\beta(^{32}O_2)}{\beta(^{34}O_2)} \cong \frac{\beta_1(^{32}O_2)}{\beta_1(^{34}O_2)}$ and $\frac{\beta(^{32}O_2)}{\beta(^{34}O_2)} \cong \frac{\beta_1(^{32}O_2)}{\beta_1(^{34}O_2)}$ one can state that the exchange between the β and β_1 states occurs much more readily than between the β_1 and β_2 states. Then, in

the general case, scheme I, which is valid for the low O_2 pressures, can be represented as follows:

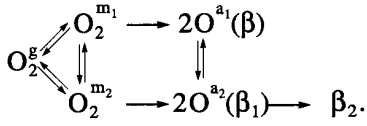

(II)

The irreversibility of the last step demonstrates difficulties in the exchange between the high-temperature states of oxygen. This scheme, more exactly, its fragment $\beta \rightleftharpoons \beta_1 \longrightarrow \beta_2$ is in good agreement with the data obtained in [31], where the dynamics of the transfer of an oxygen label was studied in a reaction mixture with a constant composition. In particular, it was found that the electrophilic "epoxidizing" oxygen (β_2) was formed from the nucleophilic oxygen (β) via an intermediate subsurface state. The latter was in equilibrium with the β state of oxygen, so that these states cannot be distinguished isotopically. In addition, the exchange between electrophilic and subsurface oxygen was also hampered, which agrees well with the results obtained in this work. Therefore, one can assume that the β_1 state is due to the oxygen penetrating into subsurface silver layers. However, this oxygen is unlikely to be dissolved, because in this case, a continuous wide peak typical of diffusion processes could be observed. Most probably, the β_1 state results from the formation of rather stable oxide-like structures involving Ag atoms from the defective phase.

Oxygen TD spectra of activated catalysts were quite similar to those of freshly prepared samples obtained after oxygen adsorption at high pressures and temperatures (Fig. 5). This allowed us to conclude that virtually the same states of oxygen were formed at lower temperatures under the action of the reaction mixture. This is in good agreement with the conclusions made in [28, 30], where analogous studies were performed with bulk silver samples.

On the basis of experimental data obtained, the sharp dependence of the epoxidation rate on the size of silver particles can be explained as follows. As the particle size decreased, especially when $d < 500$ Å, the rate of oxygen dissociative adsorption drastically dropped to form the β state or subsurface oxide $Ag^+ \diagdown O^{2-} \diagup Ag^+$. As a result, this led to a significant decrease in the concentration of silver cations capable of activating ethylene as its π-complexes with Ag^+, an intermediate in the epoxidation reaction [18]. This resulted in an abrupt decrease in the rate of ethylene epoxidation, which was proportional to the fraction of the regular surface.

The main results of this work are the following.

(1) Several states of oxygen thermal desorption were revealed on the supported silver catalysts, those are (1) the molecular α state with $T_{max} = 350$ K, (2) the atomic β state with $T_{max} = 560$–580 K, the β_1 state with $T_{max} = 600$–620 K, and the β_2 state with $T_{max} = 670$–700 K. It was found that for silver particles with a size larger than 500 Å, the last two states were formed only at elevated temperatures and oxygen pressures and, evidently, were due to the defective surface layers of silver.

(2) For Ag particles < 500 Å, a sharp decrease in $S_{0,\beta}$ and an increase in θ_α caused by a drastic increase in the silver defectivity were found. The coverage of molecular oxygen may serve as a measure of defectivity of the Ag particle surface.

(3) The kinetic scheme was suggested for describing the formation of different oxygen states on silver with the account made for the change of its structural characteristics with a change in the particle size. The quantitative description of temperature dependences of the initial sticking coefficient of oxygen with the formation of the atomic state was obtained for low oxygen pressures.

(4) The correlation was revealed between the adsorption rate of oxygen forming the β state and the rate of ethylene epoxidation. This correlation supported the previous data on the necessity of regular silver states for the activation of ethylene.

ACKNOWLEDGMENTS

This work was supported by the Russian Foundation for Basic Research (project no. 93-03-04821 and no. 94-03-08284) and by the International Science Foundation (grant no. RP 8000).

APPENDIX

Calculation of the Parameters of Kinetic Scheme I

In our calculations, we assumed that the total number of adsorption surface centers of the I and II types was equal to 5.67×10^{18} m^{-2} [3].

Because molecular α-oxygen was adsorbed only on defective sites of the silver surface, and the coverage of β-oxygen over the small particles at T_{ads} was almost three times less than the coverage of α-oxygen, it was reasonable to take the fraction of the surface of II type (n_{II}) for these particles equal to 0.75. The fraction of the surface of the second type for the larger particles (560 and 1000 Å) will be five and ten times lower, i.e., it will be 0.15 and 0.07, respectively. The values of n_I were determined from the formula $n_I = 1 - n_{II}$.

All rate constants were expressed in a standard way: $k = \nu \exp(-E_a/RT)$. Activation energies of desorption, $E_{des}^{m_1}$, and adsorption, $E_{ads}^{m_1}$, for the molecular state on the surface of I type were set equal to 50 and 12 kJ/mol, respectively [3]. For sites of II type, $E_{des}^{m_2}$ was taken equal to 92 kJ/mol. $E_{ads}^{m_1}$ equal to ≈12 kJ/mol was calculated from the formula $S = C\exp(-E_{ads}^{m_2}/RT)$, where S is the initial sticking coefficient of oxygen giving the α state; C is the probability of a molecule trapping, which is 0.23 for O_2 on Ag(111) [32].

The activation energies of diffusion between molecular states were calculated by the following formulas: $E_{dif}^{m_1} = E_{des}^{m_1}/3 = 16$ kJ/mol and $E_{dif}^{m_2} = (E_{des}^{m_2} - E_{ads}^{m_2}) - (E_{des}^{m_1} - E_{ads}^{m_2}) + E_{dif}^{m_1} = 66$ kJ/mol. For diffusion between atomic states, activation energies were found by the formula $E_{dif}^{a_1} = E_{dif}^{a_2} = E_{des}^{a_1}/3 = 59$ kJ/mol, in which $E_{des}^{a_2}$ and $E_{des}^{a_1}$ were taken independent of the coverage and equal to 176 kJ/mol. Note that the final result appeared to be insensitive to up to 10% of change in $E_{des}^{a_2}$ and $E_{des}^{a_1}$.

Oscillation frequencies of adsorbed atoms and molecules were set equal to $\nu^a = \nu^m = 10^{13}$ s^{-1} [3]. In the estimation of diffusion preexponential factors, we proceeded from the following model of the relative position of regular sites and defects on the surface. Adsorption centers were located in the nodes of a square lattice. It was assumed that the adsorption sites of the type, which occupied less than half the surface and was denoted as B (the other type was designated as A), were clustered in islands of a certain size consisted of $N \times N$ atoms. Then, the mean fraction of neighboring sites of A type along the boundary with the centers of B type will be $4N/4N^2 = 1/N$. The mean fraction of neighboring sites of A type adjacent to the sites of B type will be expressed by the formula $4N/4N^2(n_A/n_B) = n_B/Nn_A$, where n_A and n_B were the fractions of centers A and B, respectively. Hence, the preexponential factors in the expressions for the diffusion constants of molecules and atoms moving from centers B to centers A will be ν^m/N and ν^a/N, respectively. For the diffusion in the opposite direction, i.e., from A to B, the diffusion constants will be $\nu^m n_B/Nn_A$ and $\nu^a n_B/Nn_A$. It appeared that the final result was insensitive to the variation of N, because the standard deviation σ changed by less than 5% with an increase in N^2 from 1 to the maximum possible value equal to $n_B N_{surf}$, where N_{surf} was the number of atoms on the surface.

For simplicity, no allowance was made for the dissociation of oxygen molecules at the boundaries between regular and defective sites of the surface.

The calculation was performed by the above kinetic scheme using the implicit method and formulas for reverse differentiation [33]. The remaining parameters, $E_{dis}^{m_1}$, $E_{dis}^{m_2}$, $\nu_{dis}^{m_1}$, $\nu_{dis}^{m_2}$, were determined by the least-squares method so that the calculated and experimental values of $S_0(T)$ were in close agreement (σ was about 15%). The energies chosen with an accuracy of 0.5 kJ/mol were $E_{dis}^{m_1} = 49.5$ and $E_{dis}^{m_2} = 73$ kJ/mol. The oscillation frequencies $\nu_{dis}^{m_2} = 3.2 \times 10^6$ s^{-1} for all particles and $\nu_{dis}^{m_1} = 1.9 \times 10^{11}, 2.2 \times 10^{10}$, and 1.2×10^{10} s^{-1} for the particles with d = 160, 560, and 1000 Å, respectively. The fact that $\nu_{dis}^{m_1}$ was much greater than that for the Ag(111) plane (1.7×10^7 [3]) may be explained by a higher concentration of defects on dispersed silver as compared to the single crystal surface.

REFERENCES

1. Engelgardt, H.A. and Menzel, D., *Surf. Sci.*, 1976, vol. 57, no. 1, p. 59.
2. Grant, R.B. and Lambert, R.M., *Surf. Sci.*, 1984, vol. 146, nos. 2–3, p. 256.
3. Campbell, C.T., *Surf. Sci.*, 1985, vol. 157, no. 1, p. 43.
4. Bowker, M., Barteau, M., and Madix, R.J., *Surf. Sci.*, 1980, vol. 92, nos. 2–3, p. 528.
5. Haul, R., Neubauer, G., Fisher, D., *et al., Proc. 8th Int. Congr. on Catalysis,* Berlin, 1984, vol. 5, p. 265.
6. Bukhtiyarov, V.I., Boronin, A.I., Prosvirin, I.P., and Savchenko, V.I., *J. Catal.,* 1994, vol. 150, no. 2, p. 268.
7. Bowker, M., Pudny, P., and Roberts, G., *J. Chem. Soc., Faraday Trans. 1,* 1989, vol. 85, no. 8, p. 2635.
8. Dean, M. and Bowker, M., *Appl. Surf. Sci.*, 1988–1989, vol. 35, no. 1, p. 27.
9. Sobyanin, V.A., Gorodetskii, V.V., and Bulgakov, N.N., *React. Kinet. Catal. Lett.*, 1975, vol. 3, no. 2, p. 223.
10. Albers, H., van der Wal, W.J.J., and Bootsma, G.A., *Surf. Sci.*, 1977, vol. 68, no. 1, p. 47.
11. Kondarides, D.I. and Verykios, X.E., *J. Catal.*, 1993, vol. 143, no. 2, p. 481.
12. Dean, M. and Bowker, M., *J. Catal.,* 1989, vol. 115, no. 1, p. 138.
13. Kitson, M. and Lambert, R.M., *Surf. Sci.,* 1981, vol. 109, no. 1, p. 60.
14. Rehren, C., Isaac, G., Schlögl, R., and Ertl, G., *Catal. Lett.,* 1991, vol. 11, no. 3, p. 253.
15. Meima, G.R., Vis, R.J., van Leur, M.G.J., *et al., J. Chem. Soc., Faraday Trans. 1*, 1989, vol. 85, no. 2, p. 279.
16. Grant, R.B. and Lambert, R.M., *J. Catal.*, 1985, vol. 92, no. 2, p. 364.
17. Rigas, N.C., Svoboda, G.D., and Gleaves, J.T., *Catalytic Selective Oxidation*, Osyama, S.T. and Hightower, J.W., Eds., ACS Symp. Series, 1993, vol. 14, p. 183.
18. Goncharova, S.N., Paukshtis, E.A., and Bal'zhinimaev, B.S., *Appl. Catal.*, 1995, vol. 126, no. 1, p. 67.
19. Mastikhin, V.M., Goncharova, S.N., Tapilin, V.M., *et al., J. Mol. Catal. A: Chemical*, 1995, vol. 96, no. 1, p. 175.
20. Tsybulya, S.V., Kryukova, G.N., Goncharova, S.N., *et al., J. Catal.,* 1995, vol. 154, no. 1, p. 194.
21. Bukhtiyarov, V.I., Prosvirin, I.P., Kvon, R., *et al., J. Phys. Chem.* (in press).
22. Kaye, G.W. and Laby, T.H., *Tables of Physical and Chemical Constants,* London: Longmans. Translated under the title *Tables of Physical and Chemical Constants*, Moscow: Fizmatgiz, 1962.
23. Vasil'ev, L.L. and Tanaeva, S.A., *Teplofizicheskie svoistva poristykh materialov* (Thermal Properties of Porous Materials), Minsk: Nauka i Tekhnika, 1971.
24. Readhead, P.A., *Vacuum*, 1962, vol. 12, no. 1, p. 203.

25. Bowker, M., *Surf. Sci.*, 1980, vol. 100, no. 3, p. L472.

26. Zhdanov, V.P., *Surf. Sci.*, 1983, vol. 133, nos. 2–3, p. 469.

27. Backx, C., de Groot, C.P.M., and Biloen, P., *Surf. Sci.*, 1981, vol. 104, no. 1, p. 300.

28. Bukhtiyarov, V.I., Boronin, A.I., Savchenko, V.I., *J. Catal.*, 1994, vol. 150, no. 2, p. 262.

29. Pai, W.W., Bartelt, N.C., Peng, M., and Reutt-Robey, J.E., *Surf. Sci.*, 1995, vol. 330, no. 3, p. L679.

30. Bukhtiyarov, V.I., Prosvirin, I.P., and Kvon, R.I., *Surf. Sci.*, 1994, vol. 320, nos. 1–2, p. L47.

31. Bulushev, D.A. and Bal'zhinimaev, B.S., *Kinet. Katal.*, 1996, vol. 37, no. 1, p. 149.

32. Spruit, M.E.M., Kuipers, E.W., Geuzerberg, F.H., and Kleyn, A.W., *Surf. Sci.*, 1989, vol. 215, no. 3, p. 421.

33. Arushanyan, O.B. and Zaletkin, S.F., *Chislennoe reshenie obyknovennykh differentsial'nykh uravnenii na fortrane* (Numerical Solution of Ordinary Differential Equations in Fortran), Moscow: Mosk. Gos. Univ., 1990.